Peak-to-Average Power Ratio Reduction for OFDM Modems

J.Akhtman, B.Z.Bobrovsky and L.Hanzo
Dept. of ECS., Univ. of Southampton, SO17 1BJ, UK.
Tel: +44-23-80-593 125, Fax: +44-23-80-593 045
Email: lh@ecs.soton.ac.uk, http://www-mobile.ecs.soton.ac.uk

Abstract— **A novel technique of reducing the Peak-to-Average Power Ratio (PAPR) of Multi-Carrier (MC) modulated signals is proposed. The method advocated is spectrally efficient, has a low implementational complexity and hence it is also suitable for low-power, portable implementation. Moreover, it was designed to be compatible with existing standard-based Orthogonal Frequency Division Multiplex (OFDM) systems. As an example of the performance of the proposed scheme, the amplifier back-off requirement in a Terrestrial Digital Video Broadcast (DVB-T) system can be reduced from 12 to 6 dB, while satisfying the of out-of-band emission specifications imposed by the Federal Communications Commission (FCC) spectral mask.**

I. Introduction

Multi-Carrier (MC) modulation techniques [1] and in particular Orthogonal Frequency Division Multiplexing (OFDM) [1], constitute efficient modulation schemes, which are suitable for wireless broadband communications. In recent years several industrial standards based on OFDM have emerged, such as the Terrestrial Digital Video Broadcast (DVB-T), the IEEE 802.11 Wireless Local Area Network (W-LAN) scheme, as well as the IEEE 802.16 Broadband Wireless Access (BWA) standard. An impediment, limiting the extensive employment of these systems is their relatively high implementational cost, which is a consequence of requiring high-linearity, class A amplifiers having a low power-efficiency. This requirement is imposed by the high Peak-to-Average Power Ratio (PAPR) of the OFDM signal, potentially resulting in non-linear distortions producing upper harmonics of the signal and associated out-of-band emissions [2,3]. Since the most problematic non-linear component within the transmission chain is the Power Amplifier (PA), in this treatise we will focus our attention on this component.

The most straightforward method of mitigating this problem is the introduction of an amplifier 'back-off', implying that the PA is configured to operate at a certain power, which provides a sufficiently high head-room for the high modulated signal peaks to be amplified without clipping. This allows the entire input signal to be amplified within the PA's linear range. Naturally, this back-off, results in an inefficient operation of the PA. In some systems the power back-off requirements are as high as 12dB. In terms of system costs, this translates into requiring a more than 10 times more powerful PA, which may be significantly more expensive. Therefore, the only attractive solution for improving the cost efficiency of MC systems is the reduction of the PAPR of the signal. Numerous studies have been published in recent years [1], which had the potential of providing various alternative solutions for mitigating the PAPR problem. However, only a few of them have found their way into practical implementations. Some examples of previously proposed solutions, along with their associated difficulties are as follows.
1. The introduction of a spectral guard band has the potential of preventing the spectral spillage into adjacent bands and hence mitigates the associated power back-off as well as linearity requirements. However, this approach is spectrally inefficient.
2. The employment of specific coding schemes reducing the PAPR [4–6] affects the design of the Forward Error Correction (FEC) coding scheme and hence may reduce the efficiency of the FEC code, as well as the effective throughput, since they introduce redundancy by setting the parity bits of the associated block codes, such that they minimise the PAPR. Moreover, it is not a trivial task to find appropriate PAPR reduction codes for systems having a large number of subcarriers.
3. Clipping and filtering the modulated signal [7,8], as well as employing peak windowing [8,9] are closely related to the technique proposed in this study, although the previously proposed techniques may introduce severe in-band distortions of the modulated signal.
4. The set of distortionless techniques proposed in [10,11] may increase in importance for employment in future systems, although they exhibit a high complexity.

The basic requirements of practical PAPR reduction techniques are as follows:

- Compatibility with the family of existing modulation schemes;
- High spectral efficiency;
- Low complexity.

The technique proposed in this contribution was designed for satisfying the above requirements. The proposed method is closely related to [8], but has several significant improvements, which render it more suitable for practical implementations. The proposed approach may be viewed as an extension of the solutions advocated in [2,7–9,11].

The rest of this treatise is organised as follows. Section II characterises the MC signal's amplitude statistics. The impact of non-linear distortions on the transmitted signal, namely on its waveform and spectral properties are also considered. In section III a brief outline of a generic OFDM transmitter is given and the proposed PAPR reduction technique is described. Section IV provides our performance study in the context of a particular DVB-T system scenario.

II. PAPR properties of MC signals

The non-linear distortion effects imposed by the PA manifest themselves as a reduction of the signal amplitude peaks according to the PA's Amplitude to Amplitude (AM/AM) conversion characteristic. A typical AM/AM transfer characteristic can be seen in Figure 1. The intercept point in the figure indicates the so-called 1dB compression point, where the output power level is 1dB below the expected linear transfer function as a consequence of the compression of high output signal peaks.

The power of the distortion products produced by the PA is often defined as the amount of signal energy fed into the PA in excess of that corresponding to the 1dB compression point. This quantity may be further characterised by the Peak-to-Average Power Ratio (PAPR) properties, i.e. by quantifying the statistical deviation of the input signal power peaks from the Root Mean Square (RMS) power. The signal's PAPR properties can also by characterised by the Threshold Crossing Probability (TCP), i.e. by the probability that the signal amplitude exceeds a certain threshold level. The TCP plot recorded for several single carrier modulation schemes and for a 1024-subcarrier OFDM scheme is depicted in Figure 2.

The financial support of the Virtual Centre of Excellence, UK is gratefully acknowledged.

0-7803-7757-5/03/$17.00 ©2003 IEEE.

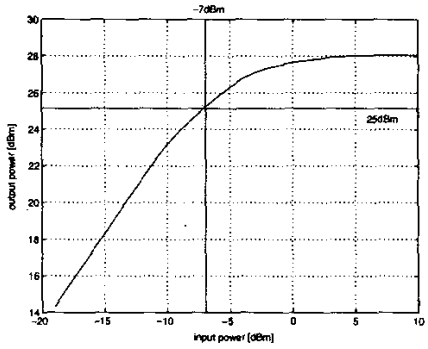

Fig. 1. Typical amplifier output versus input power response

In case of OFDM the transmitted baseband signal may be represented as:

$$s(t) = \sum_{k=0}^{K-1} (a_k + jb_k) \exp(-j2\pi\omega_k t), \qquad (1)$$

where K is the number of subcarriers, while a_k and b_k are the real and imaginary components of the complex modulating symbols of the K subcarriers, respectively. For example, for 16-QAM modulation a_k and b_k may assume the equiprobable values of $\{-3, -1, 1, 3\}$. From the central limit theorem it follows [8] that for large values of K (in practice for K exceeding 64), both the real and imaginary component of $s(t)$ becomes a normally distributed variable having a mean of zero. Hence the amplitude of the complex baseband OFDM signal (for $K > 64$) is complex Gaussian, or - synonymously - Rayleigh distributed. The distribution of the instantaneous power level hence becomes a central chi-square distribution with two degrees of freedom. In tangible physically interpreted terms the high PAPR is a consequence of the constructive superposition of high subcarrier values of numerous subcarriers.

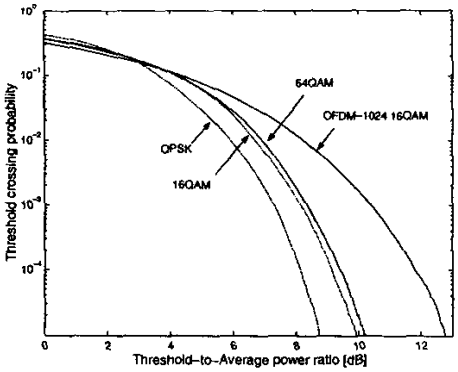

Fig. 2. Signal power Threshold Crossing Probability (TCP) versus the threshold level for 4, 16 and 64 QAM single carrier modulation schemes and for 1024-subcarrier OFDM. The RMS value of all the signals was normalized to unity.

III. Crest-Factor Reduction

A. The Principle

The impact of the amplifier-induced non-linear distortions manifests itself as:
1. in-band waveform distortion, resulting in a Signal-to-Noise Ratio (SNR) degradation, and
2. out-of-band emission of high-order non-linear distortion products resulting in adjacent channel interference.

The relative importance of these effects varies in the context of different applications according to the particular SNR and out-of-band emission requirements of the system considered. However, in most practical cases the out-of-band emission is the limiting factor, which defines the amplifier back-off requirements.

The square-root Nyquist-shaped transmit filter of multi-carrier systems, such as OFDM, typically exhibits a low Nyquist roll-off factor. In the transition-band of the transmit filter typically virtual subcarriers are allocated, which carry no useful information. Additionally, often a certain frequency domain guard band is used for eliminating the potential adjacent-channel interference, hence the transmit and receive filtering does not distort the frequency domain modulated signal. The proposed PAPR reduction technique employs this frequency domain guard band for accommodating the spectrum of an appropriately designed clipping signal, which assists in reducing the PAPR of the OFDM signal. This clipping signal is designed such that the in-band distortion imposed by the clipping procedure is minimised. The idea of using a fraction of the useful data-bearing subcarriers for carrying a signal which reduces the PAPR was previously introduced in [11]. The philosophy of employing these redundant PAPR-reduction subcarriers may be interpreted as the equivalent of using the previously mentioned block-coding scheme, which incorporates redundant bits in the time domain. However, the solution advocated in [11] was computationally demanding, and it was unsuited for employment in numerous standardised OFDM systems, such as DVB-T. Our proposed method adopts a different approach, as it will be outlined in the next section.

B. Generic OFDM Transmitter Structure

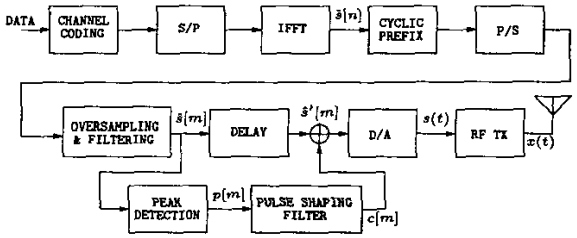

Fig. 3. Detailed OFDM transmitter explicitly showing the PAPR reduction blocks

Let us consider a generic channel coded OFDM system, including the proposed PAPR reduction block, as depicted in Figure 3. The IFFT block of Figure 3 produces the complex discrete baseband signal of

$$\check{s}[n] = \sum_{k=0}^{K-1} (a_k + jb_k) \exp j2\pi \frac{kn}{K}, \qquad (2)$$

where, again, K is the number of subcarriers, while a_k and b_k are the real and imaginary components of the complex modulating symbols, respectively. After appending the cyclic prefix this signal is then parallel to serial (P/S) converted, oversampled by a factor of I, namely by inserting $(I-1)$ zero samples after each signal sample and filtered by an interpolation filter, in order to produce the discrete complex valued signal of

$$\hat{s}[m] = \sum_{l=0}^{L-1} f[l]\, \check{s}\Big[\Big((m-l)_{div\ I} + P\Big)_{mod\ K}\Big] \cdot \delta[(m-l)_{mod\ I}], \qquad (3)$$

where m is the sample index, $f[l]$ is the l^{th} tap of an $(L+1)^{th}$ order interpolation filter, P is the cyclic prefix duration expressed in terms of the number of samples before oversampling, while $\delta[\ ]$ is the Kronecker delta function. The signal $\hat{s}[m]$ is then fed into the Digital to Analogue Converter (D/A) of Figure 3 for generating the analogue baseband signal $s(t)$. The in-phase and quadrature-phase signals are used for conveying the real and imaginary components of the complex baseband signal. The analogue baseband signal $s(t)$ is first up-converted to the intermediate frequency, producing a real-valued analogue pass-band signal. Finally, the resultant signal is fed into the Radio Frequency (RF) transmitter (TX), where it is up-converted to the desired RF carrier frequency and amplified.

The resultant real signal $x(t)$ at the input of the PA may be represented as:

$$x(t) = \Re\Big\{ s(t) \exp\left(j2\pi f_c t\right) \Big\}, \tag{4}$$

where $\Re\{\}$ represents the "real part of $\{\}$", f_c is the frequency of the carrier and $s(t)$ represents the complex envelope of the modulated signal $x(t)$.

C. Crest-Factor Reduction Algorithm

The proposed algorithm is aiming for detecting and removing the high instantaneous signal power peaks, before the signal is fed into the RF transmission chain. More explicitly, we endeavoured to remove the power peaks exceeding a certain power threshold of C^2, by clipping the modulated signal envelope peaks satisfying the condition

$$x^2(t) > C^2. \tag{5}$$

Since in Eq. 4 we have $\exp\left(j2\pi f_c t\right) \leq 1$, it may be inferred that for $x^2(t) > C^2$ we have $|s(t)| > C$. Therefore the appropriate point to include the peak detection and clipping arrangement within the transmitter schematics of Figure 3 would be at the output of the oversampling and interpolation filtering stage, producing the signal $\hat{s}[m]$.

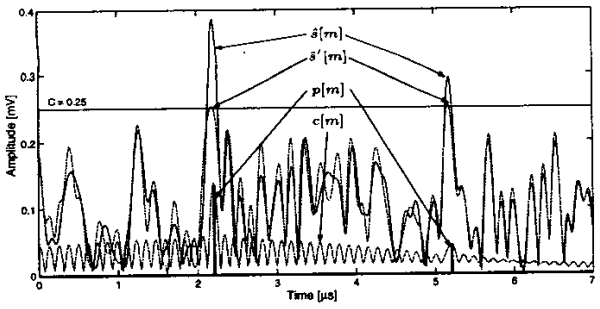

Fig. 4. Snapshots of the original OFDM signal $\hat{s}[m]$, the pulse sequence $p[m]$, the filtered clipping signal $c[m]$, and the resultant OFDM signal $\hat{s}'[m]$, generated after the PAPR reduction stage of Figure 3. The clipping threshold level of $C = 0.25$ is also shown.

Naturally, first the high peaks have to be detected. The goal of this task is to analyse the baseband OFDM signal and to identify the amplitude peaks exceeding the voltage threshold level C. This produces an oversampled signal sample sequence constituted by the signal peaks exceeding C in the following form:

$$p[m] = \sum_i \left(\hat{s}[m] - C\right)\delta[m - m_i], \tag{6}$$

where i is the non-uniformly spaced sample index running over the specific set of samples, which exceed the threshold C. These non-uniformly spaced index values m_i are defined by

$$\hat{s}[m_i] = \max_{m_i' \leq m \leq m_i''} \{\hat{s}[m]\}, \tag{7}$$

where $s[m_i']$ represents a sample on the rising edge of the signal, where it first exceeds the threshold C, while $s[m_i'']$ is a sample, where the signal peak dips below the threshold C following an excursion above it. The resultant pulse sequence $p[m]$ is depicted in Figure 4 with the aid of the black bars at positions of approximately $2.2\mu s$ and $5.2\mu s$, respectively.

The pulse sequence $p[m]$ is then processed by a shaping filter. The design of an appropriate shaping filter will be discussed in Section III-D. In case of an L^{th} order Finite Impulse Response (FIR) filter having an impulse response $f[l]$, the filtered clipping signal $c[m]$ can be expressed as the convolution of $f[l]$ and $p[m]$, yielding:

$$c[m] = \sum_{l=0}^{L-1} f[l]p[m-l]. \tag{8}$$

Finally, the filtered clipping signal $c[m]$ is synchronised with and subtracted from the discrete original OFDM signal $\hat{s}[m]$, in order to produce the desired signal having a reduced PAPR as follows:

$$\hat{s}'[m] = \hat{s}[m - v] - c[m], \tag{9}$$

where v is an integer delay introduced for ensuring the appropriate time alignment of the signals. The required value of v depends on the delay of the particular shaping filter design used and on the peak detection scheme's structure. The detailed structure of the resultant OFDM transmitter is depicted in Figure 3. Snapshots of the original modulated signal $\hat{s}[m]$ of Eq. 3, the detected pulse sequence $p[m]$, that of the filtered clipping signal $c[m]$ shown in Eq. 8, as well as the resultant OFDM signal $\hat{s}'[m]$ obeying Eq. 9 can be seen in Figure 4.

D. Shaping Filter Design

The salient feature of the proposed method is the choice of the pulse-sequence shaping filter. This filter is used for shaping the discrete pulse sequence generated by the detection of the peaks of the baseband OFDM signal, which exceed the amplitude threshold C. The characteristics of the desired filter's spectral mask are defined by the out-of-band emission requirements expressed in terms of the spectral mask imposed by the Federal Commission of Communications (FCC) [12] on a particular OFDM signal's power spectral density function. The corresponding spectral masks are represented in Figure 5. Observe in Figure 5 that the OFDM signal's spectral mask was designed such that it does not fully occupy the entire pass-band of the FCC's spectral mask, leaving a guard-band of width Δf between the masks indicated by the squares and circles. The bold lines indicate the desirable spectral characteristics of the clipping signal, which again is expected to have a low Power Spectral Density (PSD) within the useful signal's band for the sake of minimising the in-band distortion of the useful signal's spectrum. The majority of the clipping signal's PSD is expected to fall within the guard band. More explicitly, by appropriately designing the clipping signal will introduce only a low in-band distortion, which is below the attenuation level A, while inflicting virtually no out-of-band emission, which must be below the attenuation level B. Thus, the spectral-domain Transfer Function (TF) of an appropriate filter is expected to comply with the spectral requirements summarised in Table I. Below we will consider an appropriate FIR shaping filter design.

E. FIR pulse sequence shaping filter design

We will commence by stipulating a frequency-domain transfer function for the pulse shaping filter, which is defined only at

TABLE I

PULSE SEQUENCE SHAPING FILTER REQUIREMENTS

1. Exhibit an attenuation of A dB within the baseband OFDM signal's transmission band, where A is a configurable system parameter, which defines the amount of in-band distortion introduced by the peak clipping process. The role of the parameter A becomes explicit in the spectral mask of Figure 5.

2. Exhibit a pass-band width of Δf having an attenuation of 0 dB at the edge of the baseband OFDM signal's transmission band.

3. Impose a stop-band attenuation of at least B dB.

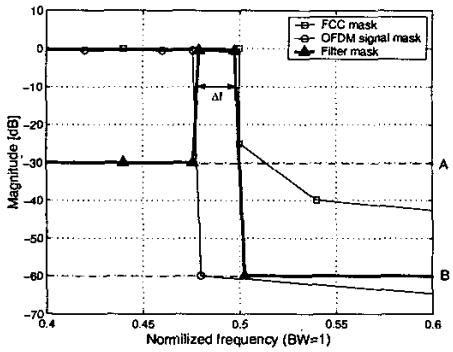

Fig. 5. Stylised spectral masks specifying the pulse sequence shaping filter. The choice of the particular parameters A and B is representative of the DVB-T system. The characteristics of the desired pulse-sequence shaping filter mask are defined by the out-of-band emission requirements imposed by the FCC, and by the DVB-T signal's power spectral density function. The bold line represents the shaping filter's transfer function requirements. It can be seen that most of the clipping signal's power is concentrated in the frequency-domain gap between the edge of the OFDM signal's spectrum and the spectral mask edge. This is necessary for ensuring that the clipping signal will introduce low in-band distortion, defined by the attenuation level A, as well as, virtually no out-of-band emission, defined by the attenuation level B.

discrete frequencies as follows:

$$G[k] = \begin{cases} A & k < k',\ k > k'' \\ 0 & k = k',\ k = k'' \\ B & k' < k < k'' , \end{cases} \tag{10}$$

where $k \in [0, I(K+P)-1]$ is a frequency domain index, representing the $I(K+P)$ number of discrete frequency-domain tones in the range $\left[-\frac{F_s}{2}, \frac{F_s}{2}\right]$, where F_s is the sampling frequency used after introducing oversampling for the sake of more accurate peak-capture. Clearly, $G[k]$ complies with the requirements of Table I, when using an appropriate choice of the values k' and k''. Furthermore, the discrete-frequency pulse-shaping filter transfer function $G[k]$ has a single-sample pass-band. The impulse response corresponding to this transfer function can be obtained by inverse Fourier transforming $G[k]$ and is given by:

$$g[l] = \frac{1}{(K+P)I} \sum_{k=0}^{(K+P)I-1} G[k] \exp j2\pi \frac{kl}{(K+P)I} , \tag{11}$$

where again, K is the number of subcarriers, P is the number of samples in the cyclic prefix and I is the previously introduced oversampling factor.

The discrete-frequency transfer function $G[k]$ is infinitely steep, having an infinite-duration impulse response $g[l]$. In order to minimise the complexity of the filtering procedure, we intend to keep the filter's order to a minimum. However, it is also desirable to mitigate the effects of the frequency-domain Gibbs oscillation imposed by using a low-order FIR filter. In order to strike a trade-off, we multiplied the FIR filter's impulse response by a time-domain windowing function, yielding:

$$f[l] = g[l] \cdot w[l] , \tag{12}$$

where $f[l]$ is the desired FIR filter's impulse response and $w[l]$ is the time-domain windowing function. In the frequency-domain the resultant FIR filter transfer function can be expressed as a convolution of $G[k]$ with the frequency response $W[k]$ of the windowing function, yielding:

$$F[k] = \sum_{m=0}^{M-1} G[k-m]W[k] . \tag{13}$$

Let us now focus our attention on the choice of the windowing function. Since according to Eq. 10 $G[k]$ has a single-sample pass-band, the bandwidth of the resultant FIR filter's pass-band will be equal to the bandwidth of the windowing function's spectral-domain main lobe. Therefore, the requirements detailed in Table I apply to the bandwidth of the windowing function's spectral-domain main lobe. Furthermore, as defined in Table I, the stop-band attenuation of the filter should be at least B dB, which imposes an additional restriction on the windowing function's spectral side-lobe attenuation. Thus, the frequency response of the desired windowing function should comply with the following requirements:

1. Have a main-lobe bandwidth of less than Δf.
2. Exhibit a side-lobe attenuation of at least B dB.

A specific windowing function, which was found to be the most suited one for our system is the Kaiser windowing function [13] given by:

$$w[l] = \frac{I_0\left(2\alpha\frac{l(L-l)}{L}\right)}{I_0(\alpha)} , \tag{14}$$

where I_0 is a zero-order modified Bessel function [14] and L is the time-domain window duration expressed in samples. The parameter α is specified by the required frequency domain side-lobe attenuation, i.e. by the filter design parameter B of Figure 5. Since the windowing function and the parameter α have been appropriately selected, the minimum window duration L and the associated minimum shaping FIR filter order are defined by the required bandwidth Δf of the main-lobe of the windowing function's frequency response.

For the specific example of the DVB-T system to be outlined in Section IV-A, the resultant filter's Kaiser-windowed impulse response can be seen in Figure 6, while the corresponding frequency-domain transfer function is represented in Figure 7. The Kaiser window used in this particular case invoked $\alpha = 8$.

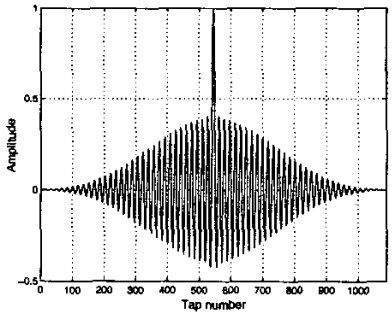

Fig. 6. FIR pulse-sequence shaping filter impulse response using Kaiser windowing and $\alpha = 8$

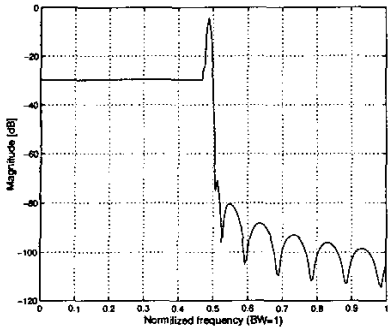

Fig. 7. FIR pulse-sequence shaping filter transfer function using Kaiser windowing and $\alpha = 8$

IV. Performance Results

A. Application in the DVB-T system

Let us now consider a practical application of the proposed PAPR reduction technique in the context of the Pan-European terrestrial video broadcast system known as DVB-T [15]. The corresponding system parameters are summarized in Table II. The out-of-band emission requirements for this application are

TABLE II
DVB-T system parameters [15].

Mode	2K
Channel bandwidth	6 MHz
Number of carriers K	1705
OFDM symbol duration T_U	298.667 μs
Carrier spacing $1/T_U$	3.3482 kHz
Effective bandwidth $(K-1)/T_U$	5.71 MHz

imposed by the Federal Communications Commission (FCC) [1] defined [12] spectral mask, which can be seen in Figure 5. A standard RF PA back-off of 12dB was defined by the DVB-T specifications, which allows the transmission of the DVB-T OFDM signal without violation of the FCC spectral mask. On the other hand, transmission with a power back-off below 12dB results in violating the FCC requirements. For example the spectrum of the DVB-T signal transmitted at a 6dB power back-off can be seen in Figure 8. However, if the proposed PAPR reduction scheme is employed, transmission at 6dB back-off can be carried out without any FCC spectral mask violation, as evidenced by Figure 8. As expected, the waveform shape of the original OFDM signal was slightly distorted, when subtracting the filtered clipping signal (see Figure 4), inflicting a moderate spectral regrowth, which can be observed in Figure 8. However, most of the spectrum of the clipping signal was concentrated within the spectral gap between the edge of the information carrying subcarriers and the FCC spectral mask of Figure 5.

As previously stated, a certain fraction of the clipping signal's power falls within the information carrying OFDM signal's bandwidth. However, the associated Signal-to-Noise Ratio (SNR) is controlled by the parameter A defined in Eq. 10 and Figure 5. In this particular case A was set to 30dB, which implies that a minimum SNR of 30dB was maintained. Thus, the clipping-induced degradation of the Bit Error Rate (BER) performance may be considered insignificant. For example, when an Additive White Gaussian Noise (AWGN) source having an SNR level of 40dB was employed, the SNR detected at the receiver was found to be 32dB.

In summary, the pulse-sequence shaping filter employed in this particular application was designed following the approach represented in Section III-E. The resultant filter's impulse response was shown in Figure 6, while the corresponding frequency-domain transfer function was depicted in Figure 7. We have demonstrated that the proposed method is appealing both in terms of its PAPR-reduction performance and its implementational simplicity.

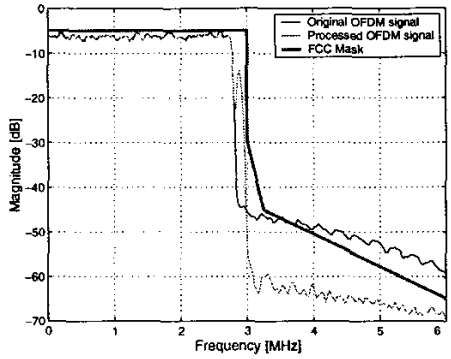

Fig. 8. Power Spectral Density (PSD) functions of both the original 2K mode, 6 MHz bandwidth, DVB-T signal transmitted using a 23dB gain RF power amplifier having a 6dB power back-off, as well as that of the same signal processed by the proposed PAPR reduction algorithm. The spectral mask defined by FCC, imposing the out-of-band emission requirements for the DVB-T transmission is also shown.

[1] The original out-of-band emission specifications for DVB-T are defined by the ETSI [15], however we used the closely-related FCC spectral mask [12], which is somewhat more stringent.

References

[1] L. Hanzo, M. Münster, B. Choi, and T. Keller, *OFDM and MC-CDMA*. John Willey - IEEE Press, May 2003.

[2] A. Chini, Y. Wu, M. El-Tanany, and S. Mahmoud, "Hardware nonliniarities in digital TV broadcasting using OFDM modulation," *IEEE Transactions on Broadcasting*, vol. 44, pp. 12–21, March 1998.

[3] E. Costa, M. Midrio, and S. Pupolin, "Impact of amplifier nonlinearities on OFDM transmission system performance," *IEEE Communications Letters*, vol. 3, pp. 37–39, February 1999.

[4] J. Davis and J. Jedwab, "Peak-to-mean power control in OFDM, Golay complementary sequences, and reed-muller codes," *IEEE Transactions on Information Theory*, vol. 45, pp. 2397–2417, November 1999.

[5] X. Li and J. A. Ritcey, "M-sequences for OFDM peak-to-average power ratio reduction and error correction," *Electronics Letters*, vol. 33, pp. 554–555, March 1997.

[6] D. Wulich and L. Goldfeld, "Reduction of peak factor in orthogonal multi-carrier modulation by amplitude limiting and coding," *IEEE Transactions on Communications*, vol. 47, no. 1, pp. 18–21, 1999.

[7] X. Li and L. Cimini, "Effects of clipping and filtering on the performance of OFDM," in *Proceedings of IEEE VTC'97*, (Phoenix, AZ, USA), pp. 1634–1638, IEEE, 4–7 May 1997.

[8] R. van Nee and A. de Wild, "Reducing the peak-to-average power ratio of OFDM," in *IEEE VTC'98 Spring*, (Ottawa, Canada), pp. 2072–2076, May 1998.

[9] R. van Nee and R. Prasad, *OFDM for wireless multimedia communications*. London, UK: Artech House Publishers, 2000.

[10] S. H. Müller and J. B. Huber, "OFDM with reduced peak-to-mean power ratio by optimum combination of partial transmit sequences," *Electronics Letters*, vol. 33, pp. 368–369, February 1997.

[11] J. .Tellado and J. Cioffi, "Efficient algorithm for reducing PAR in multi-carrier systems," in *ISIT 1998*, (Cambridge, MA, USA), August 1998.

[12] Federal Communications Commission, *FCC Regulations*. CFR Title 47, §§21.908.

[13] J. Kaiser, "Nonrecursive digital filter design using $I_0 - Sinh$ window function," in *Proceedings IEEE Symposium on Circuits and Systems*, pp. 20–23, April 1974.

[14] W. H. Press, S. A. Teukolsky, W. T. Vetterling, and B. P. Flannery, *Numerical Recipies in C*. Cambridge University Press, 1992.

[15] ETSI, *Digital Video Broadcasting (DVB); Framing structure, channel coding and modulation for digital terrestrial television*, August 1997. ETS 300 744.